

**ORIGINAL RESEARCH PAPER**

## Investigation of Brownian Motion of CuO-Water Nanofluid in a Porous Cavity with Internal Heat Generation by Using of LTNE Model

A. Zehforoosh<sup>1</sup>, S. Hossainpour<sup>2\*</sup>

*Mechanical Engineering Department, Sahand University of Technology, Sahand, Iran.*

---

**Article history:**

Received 08/07/2015

Accepted 15/08/2015

Published online 01/09/2015

---

**Keywords:**

*Heat generation*

*local thermal non-equilibrium*

*Natural convection*

*Nanofluid*

*Brownian motion*

*Porous matrix*

---

**\*Corresponding author:**

E-mail address:

hossainpour@sut.ac.ir

Phone: +98 9144156105

Fax: +98 4133444309

**Abstract**

In this paper, the effect of the Brownian term in natural convection of CuO-Water nanofluid inside a partially filled porous cavity, with internal heat generation has been studied. It is assumed that the viscosity and thermal conductivity of nanofluid consists of a static part and a Brownian part of which is a function of temperature and the volume fraction of nanofluid. Because of internal heat generation, the two-equation model is used to separately account for the local solid matrix and nanofluid temperatures. To study the effect of Brownian term various parameters such as the Rayleigh number, volume fraction of nanofluid, porosity of the porous matrix, and conductivity ratio of porous media is examined and the flow and heat fields are compared to the results of non-Brownian solution. The results show that Brownian term reduces nanofluid velocity and make smoother streamlines and increasing the thermal conductivity leads to cooling of porous material and achieving more Nusselt. Also the greatest impact of Brownian term is in low-porosity, low Rayleigh or small thermal conductivity of the porous matrix. In addition, mounting the porous material increases the Brownian effect and heat transfer performance of nanofluid but increasing porosity up to 0.8 reduces this effect.

---

### 1. INTRODUCTION

Heat convection phenomenon in a cavity filled with porous media has attracted the attention of many researchers because of the dependency of velocity field and heat conduction and convection. Also using nanofluid in cavity is a useful method in energy

transfer reinforcement due to the reinforcement in heat transfer. The results of studying nanofluid saturated porous media filled cavity can solve many problems in electronic's cooling [1], exothermic reactions inside the reactors with porous substrate [2], management of heat convection due to buried atomic

wastes [2], effect of metabolic heat production in tissues [3], transportation of medical nanoparticles in blood [3], etc.

Sheikholeslami et al [4] examined the heat and fluid flow of CuO–water nanofluid in an enclosure with a sinusoidal wall under constant heat flux. They calculated the effective thermal conductivity and viscosity of nanofluid by Koo– Kleinstreuer [5] correlation in which effect of Brownian motion on the effective thermal conductivity is considered. They found that increasing the nanoparticles volume fraction, dimensionless amplitude of the sinusoidal wall and Rayleigh number leads to an increase in average Nusselt number. Laminar natural convection in a two-dimensional square cavity filled with a CuO-water nanofluid was numerically studied by Aminossadati and Ghasemi [6]. Their main focus on this study was to compare the heat transfer performance of two pairs of heat source-sink at different Rayleigh numbers and solid volume fraction of the nanofluid. Ghasemi and Aminossadati [7] numerically studied the natural convection in a right triangular enclosure, with a heat source on its vertical wall and filled with a CuO-water nanofluid. Their comparison between the two studies of with and without Brownian motion shows that when Brownian motion is considered, the solid volume fraction has dissimilar effects on the heat transfer rate at different Rayleigh numbers. They found that, at high Rayleigh numbers, an optimum solid volume fraction can be found, which results in the maximum heat transfer rate.

Heat transfer through a fluid-saturated porous medium in a square cavity using local thermal non-equilibrium (LTNE) model was studied by Kayhani et al [8]. They obtained a correlation for the Nusselt number by solving the governing equations which is function of conductivity ratio,

interstitial heat transfer coefficient, and Rayleigh number. Sarita Pippal and P. Bera [9] attempted to understand the influence of LTNE model on natural convective flow in a slender porous cavity. They showed that for relatively low values of thermal conduction ratio Nusselt of fluid is almost independent of inter-phase heat transfer coefficient (H). Mealey and Merkin [10] investigated temperature dependent heat generation in fluid saturated porous cavity. Their results showed that in smaller Rayleigh numbers only one vortex is generated inside the cavity and by slightly increasing the Rayleigh the vortexes were deviated towards vertical walls.

Also some researchers have investigated the partially filled porous cavities. Beckermann et al [11] numerically and experimentally tested a rectangular cavity filled with layers of porous media. They showed that fluid penetration into porous layer could totally affect the flow and thermal fields. Also, fluid penetration into the porous media highly depends on the multiplication of Rayleigh and Darcy numbers. Sathe and Tong [12] experimentally investigated a rectangular cavity with dimensional ratio of 5 to 1 which was incompletely and completely filled with nickel foam and plastic foam in a laboratory. They showed that by increasing the porous media in a layered manner from hot to cold source a minimum value for heat is achieved.

Few studies have been conducted on porous media saturated with nanofluid. Sheremet and Pop [13] numerically analyzed the steady natural convection in a square porous cavity with solid walls of finite thickness filled by a nanofluid. They found that the local Nusselt number at the solid-porous interface is an increasing function of Rayleigh number and Brownian motion parameter and a decreasing function of dimensionless

thickness of the heat-conducting solid walls. Free convection in a three-dimensional porous cavity with two isothermal vertical surfaces and adiabatic rest walls filled with nanofluid has been studied numerically by Sheremet et al [14]. They proved the former results in their previous article [13]. Also Sun and Pop [15] considered a right triangle cavity with a constant temperature heat source on vertical wall and its hypotenuse was chosen as the low temperature source. They concluded that the highest value for Nusselt number is achieved when the maximum Rayleigh number is applied or by increase in the size of heater. According to the studies conducted so far, the investigations in this regard is still primitive and using nanofluid as a heat transfer agent in the presence of a porous matrix is not older than a few years. It is noteworthy that very few studies have been conducted on porous cavities filled with nanofluid and according to the latest investigations, no studies have been conducted to clarify the role of the Brownian term on natural convection heat transfer inside a nanofluid saturated and heat generating porous cavity.

In this study the natural convection of nanofluid inside a cavity which was partially filled with porous media with internal heat generation has been investigated. Brownian term effects are considered in the all calculation and streamlines, isotherms and the Nusselt values, compared with non-Brownian state. In order to investigate the variation of Brownian term before the porous matrix, different domains of porosities, thermal conduction coefficients and volume fraction of nanoparticles were investigated and the effect of each parameter on the streamlines and isotherms and consequently energy obtained from the porous heat source has been studied.

**2. Problem description**

A schematic of the square cavity with a Porous square matrix at its center is shown in Fig. 1. The side of the cavity is denoted by  $L$  and Porous square matrix sides are  $L/2$ . The horizontal top and bottom walls are assumed to be adiabatic and impermeable. The left wall is kept at uniform temperature  $T_h$ , while, the right wall is kept at reference cold temperature  $T_c$ . Heat is also generated internally within the central porous matrix which is temperature difference dependent. Also, the cavity is filled with CuO-water nanofluid where the thermophysical properties of the base fluid and the nanoparticle are given in Table 1. It is assumed that the flow is laminar, the nanofluid is Newtonian and incompressible and base fluid and the nanoparticles are in thermal equilibrium. It is assumed that the density of nanofluid in Buoyancy term changes with the Boussinesq approximation

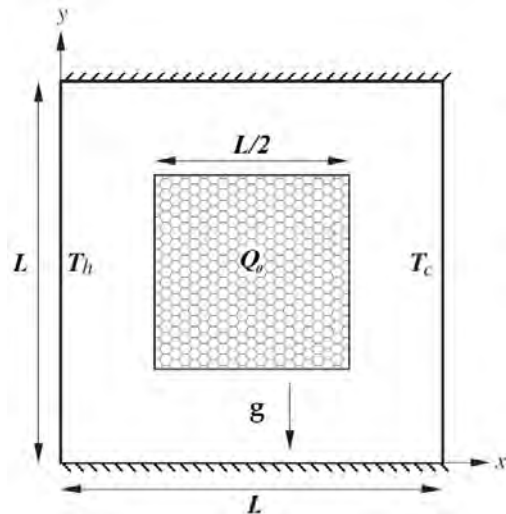


**Fig. 1.** A schematic diagram of the physical domain

**Table 1.** Physical properties of fluid and nanoparticle [6].

	$\rho$	$\mu \times 10^4$	$c_p$	$k$	$\beta \times 10^5$
	kgm <sup>-3</sup>	kgm <sup>-1</sup> s <sup>-1</sup>	Jkg <sup>-1</sup> K <sup>-1</sup>	Wm <sup>-1</sup> K <sup>-1</sup>	K <sup>-1</sup>
<b>water</b>	997.1	8.81	4179	0.613	21
<b>CuO</b>	6320	-	535.6	76.5	1.8

and both viscosity and thermal conductivity of nanofluids are functions of temperature and volume fraction. Also the porous medium is considered to be homogeneous, isotropic, non-deformable, saturated with nanofluid. Due to internal heat generation, the two-equation model is used to account for the local solid matrix and nanofluid temperatures separately. For interstitial heat transfer coefficient at pore level (H) values lower than 100 the energy gain from porous matrix is negligible and therefor in all studied cases its quantity is considered to be 100. Also in order to use the two-equation model the porosity of the value of 0.005 is used instead of solid block (zero porosity). Moreover compared to porous pore size, the dimensions of nanoparticles are very small.

### 3. Governing equation

For the partially porous cavity case, instead of solving the two sets of equations separately, the equations can be combined into one set by introducing the binary parameter  $\delta$ , which is either zero or one for nanofluid and porous regions respectively. The governing continuity, momentum and energy equations in non-dimensional form, used in this study are [11, 12, 16]:

$$\frac{\partial U}{\partial X} + \frac{\partial V}{\partial Y} = 0 \tag{1}$$

$$\left(\frac{\delta}{\varepsilon^2} - (\delta - 1)\right) \left[ U \frac{\partial U}{\partial X} + V \frac{\partial U}{\partial Y} \right] = -\frac{\partial P}{\partial X} + \frac{\mu_{nf}}{\rho_{nf} \alpha_f} \left[ \frac{\partial^2 U}{\partial X^2} + \frac{\partial^2 U}{\partial Y^2} \right] + \delta \frac{\mu_{nf}}{\rho_{nf} \alpha_f Da} U \tag{2}$$

$$\left(\frac{\delta}{\varepsilon^2} - (\delta - 1)\right) \left[ U \frac{\partial V}{\partial X} + V \frac{\partial V}{\partial Y} \right] = -\frac{\partial P}{\partial Y} \tag{3}$$

$$+ \frac{\mu_{nf}}{\rho_{nf} \alpha_f} \left[ \frac{\partial^2 V}{\partial X^2} + \frac{\partial^2 V}{\partial Y^2} \right] + \delta \frac{\mu_{nf}}{\rho_{nf} \alpha_f Da} V + \frac{\beta_{nf}}{\beta_f} Ra \tag{4}$$

$$U \frac{\partial \theta_{nf}}{\partial X} + V \frac{\partial \theta_{nf}}{\partial Y} = (\delta(\varepsilon - 1) + 1) \frac{\alpha_{nf}}{\alpha_f} \left[ \frac{\partial^2 \theta_{nf}}{\partial X^2} + \frac{\partial^2 \theta_{nf}}{\partial Y^2} \right] + \delta H(\theta_s - \theta_{nf}) \tag{5}$$

$$0 = \delta(1 - \varepsilon) R_k \frac{(\rho c)_f}{(\rho c)_{nf}} \left[ \frac{\partial^2 \theta_s}{\partial X^2} + \frac{\partial^2 \theta_s}{\partial Y^2} \right] + \delta H(\theta_{nf} - \theta_s) \tag{6}$$

In the above equation  $\varepsilon$  is the value of porosity which equals one for a nanofluid field and varies between zero and one in a porous field. Also applied non-dimensional parameters are [11, 16]:

$$X = \frac{x}{L}, Y = \frac{y}{L}, U = \frac{uL}{\alpha_f}, V = \frac{vL}{\alpha_f}, Da = \frac{K}{L^2}$$

$$Pr_f = \frac{\nu_f}{\alpha_f}, H = \frac{hL^2}{(\rho c)_{nf} \alpha_f}, q = \frac{Q_0 L^2}{\Delta T^2 (\rho c)_{nf} \alpha_{nf}}$$

$$R_k = \frac{k_s}{k_f}, P = \frac{\rho L^2}{\rho_{nf} \alpha_f^2}, \theta_f = \frac{T_f - T_c}{T_h - T_c}$$

$$\theta_s = \frac{T_s - T_c}{T_h - T_c}, Ra_f = \frac{\beta_f L^2 (T_h - T_c)}{\nu_f \alpha_f} \tag{7}$$

Organ equation [17] can be used to define the permeability of porous media, by assuming that the porous media is composed of  $d$  diameter spherical objects:

$$K = \frac{d^2 \varepsilon^3}{175(1 - \varepsilon^2)} \tag{8}$$

Where the density, heat capacity, thermal expansion coefficient of the nanofluid are [18]:

$$\rho_{nf} = \varphi \rho_p + (1 - \varphi) \rho_f \tag{9}$$

$$(\rho c)_{nf} = \varphi (\rho c)_p + (1 - \varphi) (\rho c)_f \tag{10}$$

$$(\rho \beta)_{nf} = \varphi (\rho \beta)_p + (1 - \varphi) (\rho \beta)_f \tag{11}$$

It is assumed that  $\mu_{nf}$  and  $k_{nf}$  consist of a conventional static part as well as a dynamic part which originates from the Brownian motion of nanoparticles [5, 19]:

$$\mu_{nf} = \mu_{static} + \mu_{Brownian} \tag{11}$$

$$k_{nf} = k_{static} + k_{Brownian} \tag{12}$$

The Static viscosity of the nanofluid can be estimated with the Brinkman model [20]:

$$\mu_{static} = \frac{\mu_f}{(1 - \phi)^{2.5}} \tag{13}$$

The static thermal conductivity of nanofluid can be determined by Maxwell–Garnett’s (MG model) self-consistent approximation model [21].

$$\frac{k_{static}}{k_f} = \frac{(k_p + 2k_f) - 2\phi(k_f - k_p)}{(k_p + 2k_f) + \phi(k_f - k_p)} \tag{14}$$

$\mu_{Brownian}$  and  $k_{Brownian}$  can be calculated from the kinetic theory and Stokes' flow approximation by [5, 19]:

$$\mu_{Brownian} = 5 \times 10^{-4} \lambda \phi \rho_f \sqrt{\frac{BT}{2\rho_{np}R_{np}}} f(T, \phi) \tag{15}$$

$$k_{Brownian} = 5 \times 10^{-4} \lambda \phi \rho_f c_{p,f} \sqrt{\frac{BT}{2\rho_{np}R_{np}}} f(T, \phi) \tag{16}$$

Where B is the Boltzmann constant ( $B=1.3807 \times 10^{-23}$  J/K) and,  $\rho_{np}$  and  $R_{np}$  are the density and radius of nanoparticles, respectively. For the CuO-water nanofluid, the two modeling functions  $\lambda$  and  $f$  are experimentally estimated by:

$$\lambda = 0.0137(100\phi)^{-0.9229} \text{ for } \phi \leq 1\% \tag{17}$$

$$\lambda = 0.0011(100\phi)^{-0.7272} \text{ for } \phi > 1\% \tag{18}$$

And

$$f(T, \phi) = (-6.04\phi + 0.4705)T + (1722.3\phi + 13) \tag{19}$$

for  $1\% \leq \phi \leq 4\%$  and

$$300K \leq T \leq 325K$$

The relevant dimensionless boundary conditions are given as:

$$X = 0, \quad U = V = 0, \quad \theta = 1 \tag{20}$$

$$X = 1, \quad U = V = 0, \quad \theta = 0 \tag{21}$$

$$Y = 0, \quad Y = 1, \quad U = V = \frac{\partial \theta}{\partial Y} = 0 \tag{22}$$

Also because of using a liquid fluid with very slow velocity, it is assumed that the velocity and tangential stresses in the nanofluid and porous media interfaces are continuous [11].

$$T_{nf} = T_{PM}, \quad k_{nf} \frac{\partial T}{\partial n} = k_{eff} \frac{\partial T}{\partial n} \tag{23}$$

$$U_{nf} = U_{PM}, \quad V_{nf} = V_{PM}, \quad P_{nf} = P_{PM} \tag{24}$$

$$\mu_{nf} \frac{\partial U_{nf}}{\partial n} = \mu_{eff} \frac{\partial U_{PM}}{\partial n}, \tag{25}$$

$$\mu_{nf} \left( \frac{\partial V_{nf}}{\partial n} + \frac{\partial U_{nf}}{\partial t} \right) = \mu_{eff} \left( \frac{\partial V_{PM}}{\partial n} + \frac{\partial U_{PM}}{\partial t} \right)$$

The local variation of the Nusselt number of the nanofluid on the left and right walls can be expressed as [22]:

$$Nu_L = -\frac{k_{nf}}{k_f} \left( \frac{\partial \theta_{nf}}{\partial X} \right)_{X=0} \tag{26}$$

$$Nu_R = -\frac{k_{nf}}{k_f} \left( \frac{\partial \theta_{nf}}{\partial X} \right)_{X=1} \tag{27}$$

The total dimensionless heat generation in cavity is calculated by integrating the local Nusselt number over the left and right walls.

$$Nu = \int_0^1 (Nu_L + Nu_R) dY \tag{28}$$

#### 4. Numerical procedure, Grid independency

A control volume technique employed to discretize the differential equation. For the convective and diffusive terms, a first order upwind method was used while the SIMPLE procedure was introduced for the velocity-pressure Coupling [23]. In order to investigate grid size independency, four different sets of grid systems, for a case  $Ra=10^5$ ,  $\epsilon=0.4, R_k=10$  and  $q=1000$  in different nanoparticle volume fractions were investigated and ultimately  $100 \times 100$  arrangement was chosen; such that the chosen network guarantee the independence of the results to the meshing. Table.2 presents the Sum of average Nusselt number along the hot and cold wall for five different grid sizes.

**Table 2.** Sum of average Nusselt number along the hot and cold wall for different grids.

Grid Size		60×60	80×80	100×100	120×120
Nu	$\phi = 0.00$	15.0757	14.9667	14.9071	14.9011
	$\phi = 0.02$	16.1355	16.0653	16.0394	16.0349
	$\phi = 0.04$	16.4758	16.4119	16.3755	16.3695

**5. Code validation**

Validation was done in two steps. Fig.2 compares Nusselt values for a cavity partially filled with porous media with results of Beckermann et al. [11]. Nusselt values are obtained with  $Pr=1, R_k=1$  and  $C=0.55$  and  $S$  show the space not filled with porous media along horizontal axis. Fig. 3 shows Nusselt number variation in a cavity saturated with nanofluid with different volume fraction and Rayleigh numbers obtained from our calculations and results of Aminossadati and Ghasemi [6] as can be seen maximum difference between Nusselt values observed in volume fraction 0.02 and Rayleigh of  $10^6$  with 0.8%.

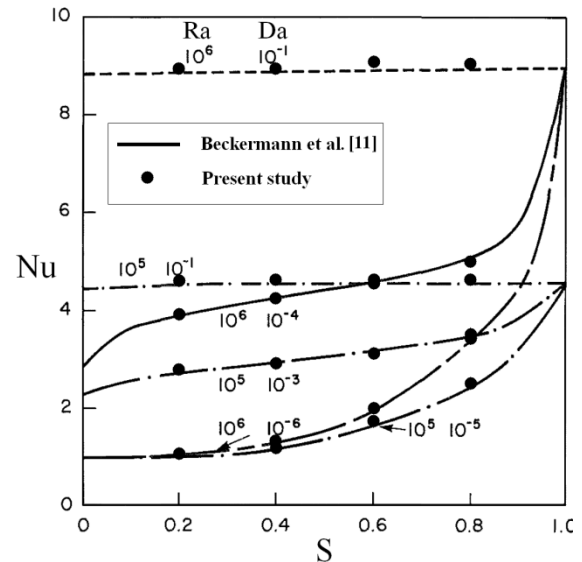


**Fig. 2.** Validation of the present code for a cavity partly filled with porous media

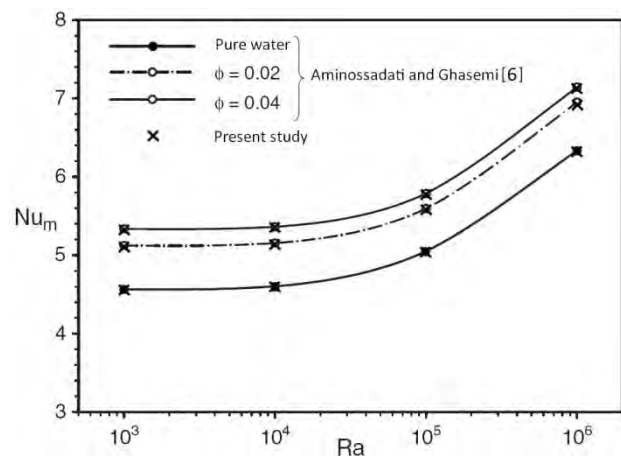


**Fig. 3.** Validation of the present code for a cavity filled with nanofluid

**6. Results**

**6.1. The effect of variation of conduction ratio in different porosities on Brownian values**

The effect of variation of conduction ratio in different porosities on isotherm and streamline contours has been considered in both presence and absence of Brownian term at  $Ra=10^5, \phi=0.04$  and  $q=1000$ . Fig. 4 shows the variations of Brownian Nusselt in different values of conduction and porosity. In lower porosities, due to the inability of the fluid to enter the porous material, the heat

generated inside the porous material can transfer out of the porous material only through thermal conduction. Therefore the values of conduction ratio play a vital role in cooling the porous material and consequently heat generation and increasing Nusselt. As can be seen increasing the conduction ratio resulted in significantly higher Nusselt values. By further increasing the porosity, the fluid could get inside the porous matrix more easily thus the heat regime was replaced with conduction heat transfer. Therefore the energy would be removed with nanofluid and in all conduction ratios the results would be almost equal and the Nusselt would be high. Interpretation of Fig. 4 has been done in detail in previous works by the authors [24] and the aim in this research is to study the effect of adding Brownian term on temperature and velocity fields and also to find the effective of domain of this term on the value of Nusselt.

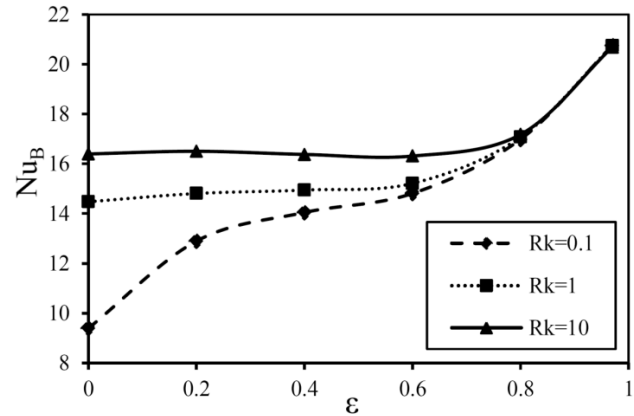


Fig. 4. Total Brownian Nusselt number for different porosities and conduction ratios at  $Ra=10^5$  and  $\phi=0.04$

Figs. 5 and 6 compare the effect of presence of Brownian term on streamlines and isotherms of the nanofluid in which the solid line shows the solution of equations with Brownian term and dashed lines are the solution without Brownian term. The total number of counters is equal for the

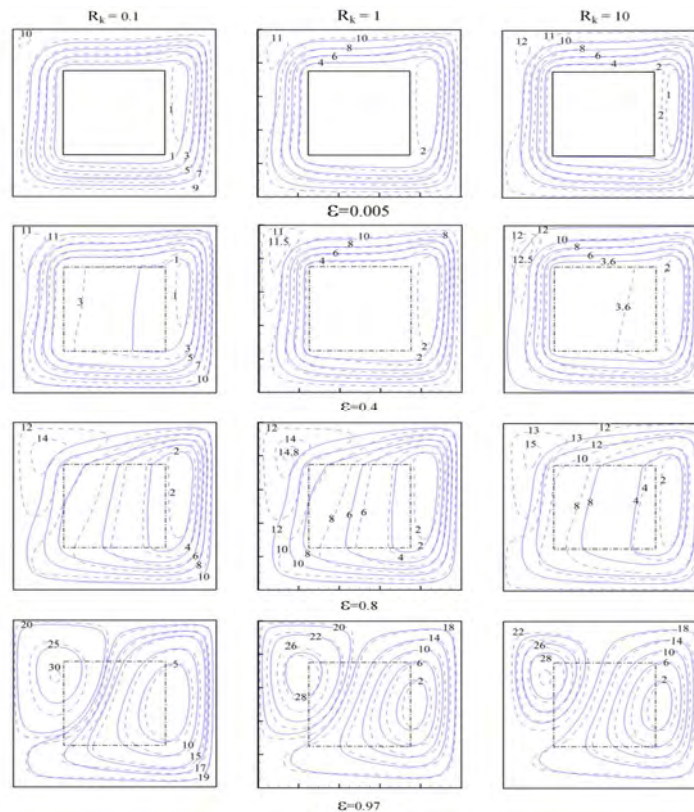


Fig. 5. Comparison of Brownian (solid) and non-Brownian (dashed) Streamlines for different conduction ratios and porosities



two states and is from minimum to maximum value of the flow function. According to Fig. 5 in the general state the increase of viscosity due to Brownian term resulted in decrease of fluid velocity values and creation of softer streamlines with lower curvature and fracture. Also in absence of Brownian it can be seen that nanofluid tends to form secondary loops even in lower porosities while in presence of Brownian there was no secondary loop observed in up left corner even in porosities up to 0.97 which is due to higher Brownian viscosity especially in upper corners.

Fig. 6 shows the isotherms for the two states. The effect of Brownian term on isotherms can be seen in the gap formed between the two lines in the Brownian and without Brownian states. In each point of the investigation in which the gap between

solid and dashed lines was bigger the Brownian term effect was higher. Brownian term resulted in increasing thermal conduction and thus cooling of the porous material and higher Nusselts. It can be seen that in zero porosity (almost zero; 0.005) at  $R_k=0.1$  the isotherms inside the block coincided therefore it is expected that the value of Brownian effect be lower but by increasing the conduction ratio the lines are opened up which indicates higher Brownian effects. By increasing the porosity in  $R_k=0.1$  it can be seen that the gap between the lines was first increased and then decreased. Also in higher porosities an almost constant pattern of lines were seen in both states which suggested an estimation of similar behavior of Brownian term in higher porosities. Another noteworthy point about the isotherms is moving the Brownian temperature

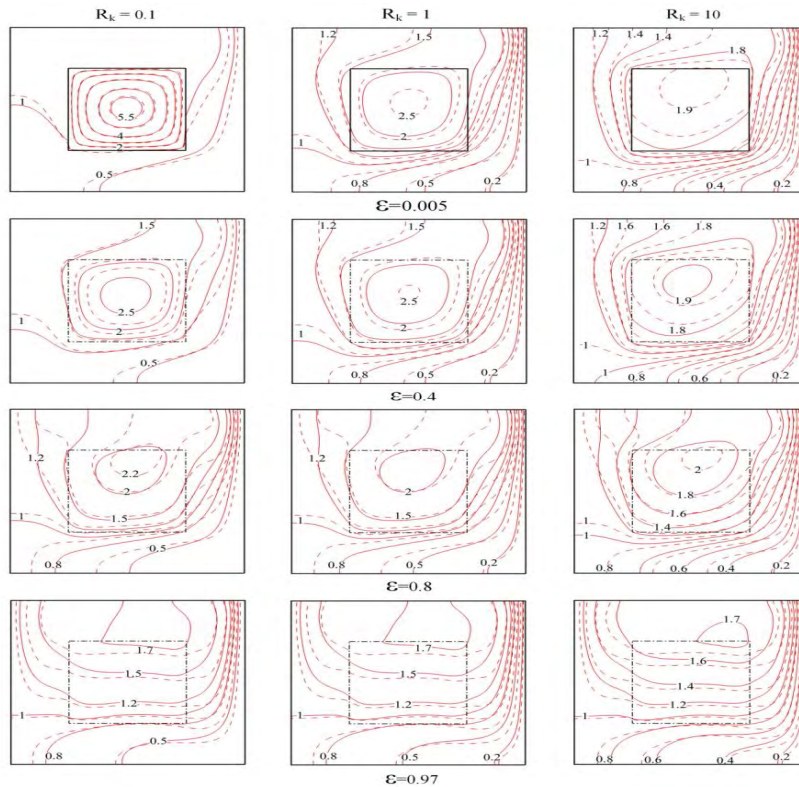


**Fig. 6.** Comparison of Brownian (solid) and non-Brownian (dashed) isotherms for different conduction ratios and porosities



lines forward on upper wall and backward on bottom wall compared to non-Brownian state. This can be related to the higher heat exchange capabilities so that nanofluid can transfer more energy to the cold wall and get more energy from the hot wall which will ultimately result in increased Nusselt values.

In order to investigate the effect of the presence of Brownian term, Nusselt factor was defined as  $Nu_B/Nu_{WB}$  which shows the Nusselt value in presence of Brownian compared to non-Brownian state. The results obtained from the investigation of this factor in different conduction coefficients and porosities are shown in Fig. 7.

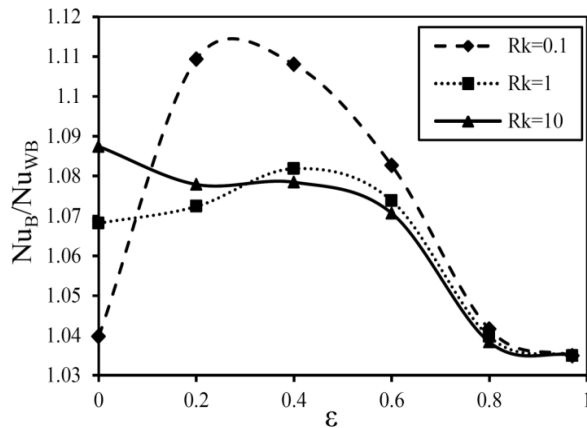


**Fig. 7.** Nusselt factor for different porosities and conduction ratios

As explained in zero porosity the fluid cannot penetrate into the block and the generated heat transfers only through conduction. Therefore in lower conduction ratios the heat is trapped inside the block and no significant change in viscosity and thermal conduction occurs in the nanofluid outside the block and Nusselt factor values remain low. But by increasing thermal conduction ratios, the energy transfers out of the block which results in increased thermal conduction through affecting the Brownian term of the nanofluid around the block, and consequently more cooling of the block and higher Nusselt values are obtained. At  $R_k=0.1$

and in all porosities, the temperature inside the porous block was higher compared to higher thermal ratios due to lower thermal conduction. This phenomenon resulted in temperature increase in the nanofluid entering the porous block and therefore increased the Brownian term and Nusselt factor compared to higher heat ratio values. On the other hand in higher porosity values, due to the relative omission of porous matrix and domination of convection regime inside the cavity (ineffectiveness of heat ratios), the block temperature decreased and therefore the Brownian term was also decreased significantly. Also, because of fluid circulation in a bigger region (middle of the chamber) the viscosity effect was added up to nanofluid flow which resulted in lower Nusselt values in all heat ratios. In this plot in porosity domain of 0.2 and 0.4 there are differences between heat ratios of 1 and 10 which is due to the domination of conduction regime in porosity of 0.2 and convection regime in porosity of 0.4. ultimately it could be concluded that in 0.8 and higher porosities good results could be obtained regardless of Brownian term but in lower porosities and especially in porous matrix with heat ratios lower than that of nanofluid (insulated matrix) Brownian term should be considered.

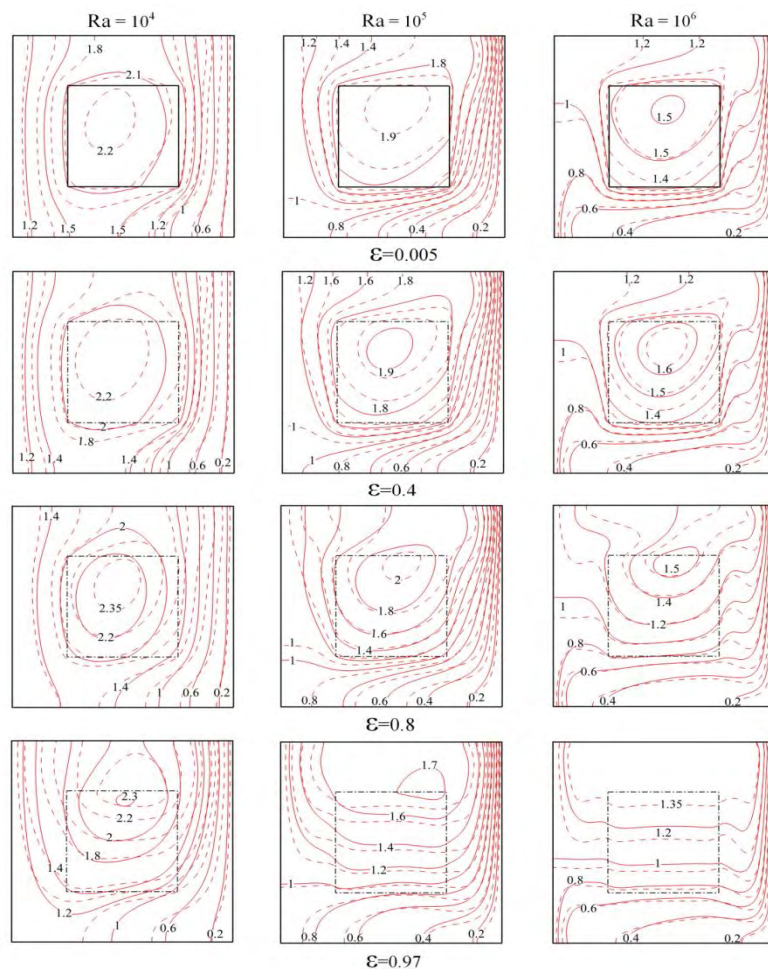
## 6.2. The effect of Rayleigh number in different porosities

The effect of variation in Rayleigh number in different porosities on temperature and velocity fields was investigated both in presence and absence of Brownian at  $R_k=10$ ,  $\phi=0.04$  and  $q=1000$ . The effect of these variations on isotherms of the nanofluid is shown in Fig. 8. From this figure it can be referred that in lower Rayleigh of  $10^4$ , due to the lower circulation velocity's of the

nanofluid, isotherms were vertical and transfer of the heat generated in the porous matrix is generally through conduction. This resulted in temperature increase in the source and consequently Brownian term increase which was obvious in the difference between the solid and dashed lines. But by increasing the porosity to the limit value of 0.97, isotherm lines became horizontal which indicated increased circulation velocity and transition to convection regime. By increasing Rayleigh the circulation velocity of nanofluid was increased and therefore more energy was obtained from the source which resulted more uniform source temperature and reduction of the gap between Brownian and non-Brownian lines (reduction of

increasing Rayleigh number in 0.97 porosity (omission of porous matrix), the gap between the solid and dashed lines inside the porous matrix was increased which was an indication of increased Brownian effect.

Fig. 9 shows the effect of variation of Nusselt factor on different Rayleigh numbers and porosities. Two different effects resulted in the current plot. The first one is the Rayleigh value whose increase resulted in faster circulation of nanofluid and therefore more sensible viscosity effect. Therefore it was observed that in lower Rayleigh values the effect of Brownian thermal conduction was higher than that of Brownian viscosity, therefore Nusselt factor values were



Brownian

**Fig. 8.** Comparison of Brownian (solid) and non-Brownian (dashed) isotherms for different Rayleigh numbers and porosities

higher in lower Rayleighs and by increasing Rayleigh more reduction was observed in Nusselt factor values. The second effect was the effect of temperature on Brownian thermal conduction and viscosity which is less significant compared to the first one; so that by increasing the Rayleigh value the temperature of the cavity was decreased and Brownian thermal conduction and viscosity values were also reduced. This was more evident in porosity of 0.97 in which the porous matrix conduction effect was removed. Due to the omission of porous matrix and total circulation of nanofluid in this porosity value, the viscosity effect was more significant than that of thermal conduction which resulted in lower Nusselt factor values in lower Rayleighs, due to the higher temperature and therefore higher viscosity in lower Rayleighs. Ultimately it could be concluded that in lower Rayleighs the Brownian effect was very high but by increasing Rayleigh the effect of Brownian term was decreased. Also the presence of porous matrix resulted in a change in temperature distribution and therefore a change in Brownian values in different Rayleighs.

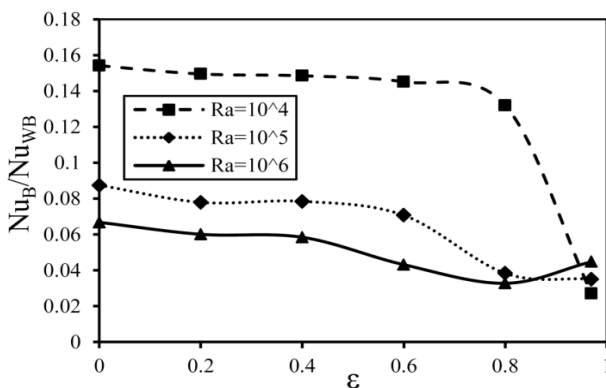
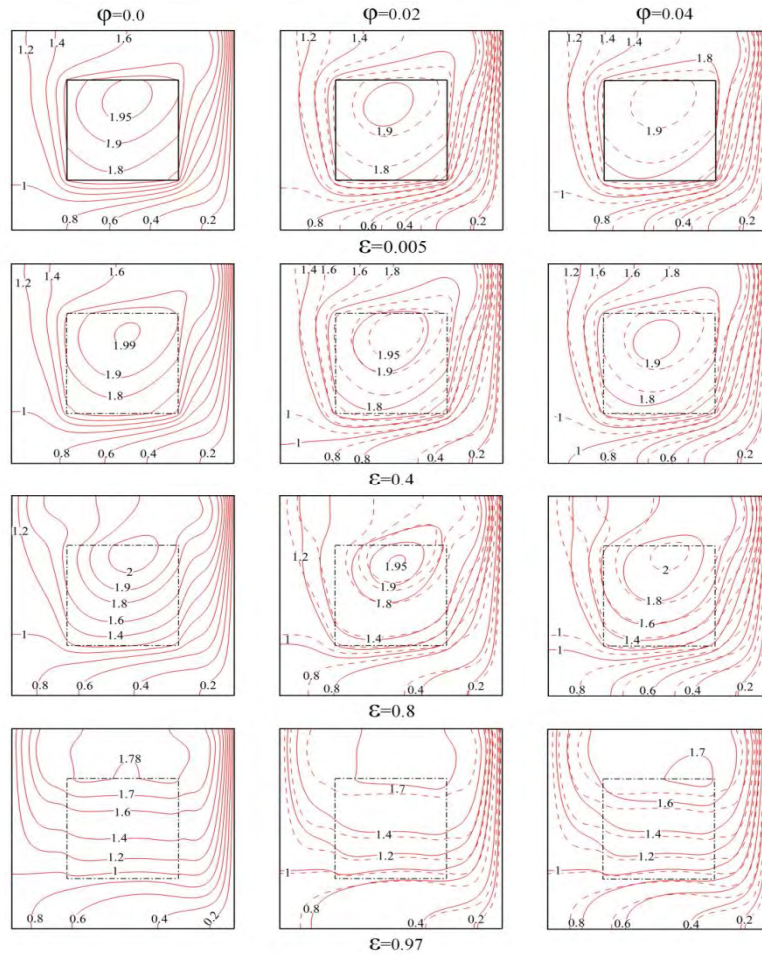


Fig.9. Nusselt factor for different Rayleigh numbers and porosities

### 6.3. The effect of volume fraction in different porosities

Addition of nanoparticles to the fluid results in a positive effect in increasing thermal conduction coefficient and negative effect in increasing viscosity in nanofluid. Fig. 10 shows these effects on isotherms in nanofluid inside the cavity. The effect of variations of nanofluid volume fraction in different porosities on temperature and velocity fields was investigated at  $Ra=10$ ,  $R_k=10$  and  $q=1000$ . By increasing volume fraction of nanofluid, thermal conduction coefficient was increased and therefore thermal reception and transmission through the nanofluid was also increased. This resulted in more temperature decrease and more heat generation and on the other hand increased vortex velocity inside the cavity. Also by increasing volume fraction the gap between the solid (Brownian) and dashed (non-Brownian) lines was also increased which showed that Brownian term increased by increasing volume fraction. In all porosities by increasing volume fraction, convection increase and maximum cavity temperature decrease were evident. On the other hand porosity increase allowed the nanofluids to enter the porous matrix and this resulted in increased convection and more energy harvest. But by increasing volume fraction, Brownian and non-Brownian isotherm lines got closed and at porosity of 0.97 almost similar patterns were observed for both volume fractions.

Fig. 11 shows that increasing the volume fraction resulted in higher Nusselt values in all porosities but the amount of this increase was more significant in lower porosities compared to higher porosities. The reason for this could be more significant effect of nanofluid viscosity on convection regime which occurs in higher porosities of the porous matrix. Once nanofluid entered the porous matrix, Darcy equation, which has a direct relation with nanofluid viscosity, is



**Fig. 10.** Comparison of Brownian (solid) and non-Brownian (dashed) isotherms for different volume fractions and porosities

inserted in the equation and higher resistance against the flow is generated. Also it can be seen that increasing volume fraction of the nanofluid resulted in non-linear Nusselt Brownian; so that the Nusselt Brownian plot for volume fraction 0.02 was closer to volume fraction of 0.04 than that of zero.

The reason for this can be near linear conformance of Brownian term with volume fraction and with degree of 1.5 related to temperature. Therefore the growth of Nusselt values in the presence of Brownian term, unlike non-Brownian state [23], would be non-linear and the temperature would have more significant role

than volume fraction in different variations due to higher capabilities.

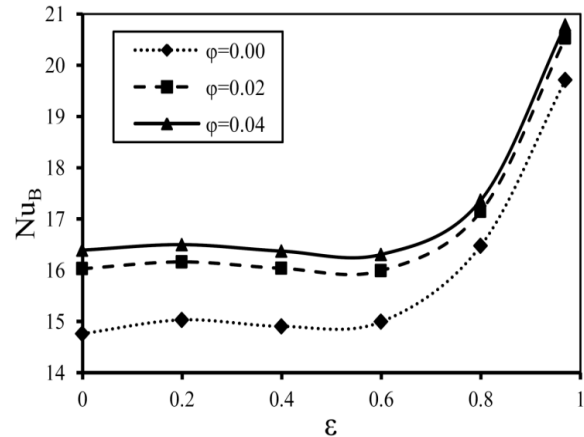


**Fig. 11.** Total Brownian Nusselt number for different porosities and volume fractions

Fig. 12 shows the Nusselt factor in different volume fractions and porosities. According to the figure it can be seen that the values of this factor was decreased by increasing porosity in both volume fractions which is firstly due to transition of the regime from conduction to convection and negative effect of viscosity increase on fluid circulation and secondly due to overall temperature decrease inside the chamber and therefore Brownian conduction value decrease in the nanofluid. Also the increase of volume fraction value resulted in increased Nusselt factor in all porosities which in lower porosities this difference was much higher but in higher porosities it approached zero. As it is explained in Fig. 11, similar flow pattern in two volume fractions was observed in higher porosities which could be due to neutralization of the effect of thermal conductivity increase with the effect of viscosity increase in higher volume fractions. In all it can be concluded that addition of porous material in all volume fractions resulted in higher contribution of Brownian in Nusselt value but by relative omission of porous matrix Brownian effect is decreased and in case the matrix was omitted the nanofluid volume fraction variation had insignificant effect on Brownian contribution.

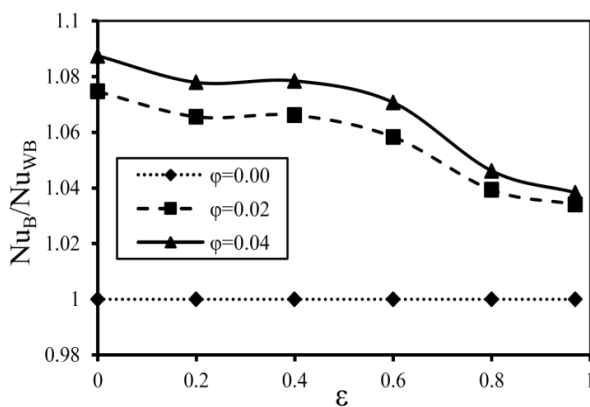


Fig. 12. Nusselt factor for different volume fractions and porosities

## 7. Conclusion

In the present study, the effect of the Brownian term in natural convection of CuO-Water nanofluid inside an enclosure which is partially filled with porous media, with internal heat generation has been studied numerically. It was assumed that the viscosity and thermal conduction of the nanofluid was a function of temperature and volume fraction of the fluid. Also in order to more precise investigation of the problem, the two-equation model is used to separately account for the local solid matrix and nanofluid temperatures.

The results showed that considering Brownian term, changed the values of viscosity and thermal conduction of the nanofluid which resulted in decreased values for the velocity of the nanofluid and softer streamlines with less curvatures and fractures. Also viscosity variations resulted in secondary vortex omission near hot wall. Brownian term resulted in increased thermal conduction and therefore cool porous material and higher Nusselts. This cooling resulted in a change in flow pattern and in the porous region, the bigger the gap between the isotherms in Brownian and non-Brownian states was the more energy received from heat source.

In all porosities the highest Nusselt factor values were obtained in the least thermal conduction which was due to the trapped heat inside the porous matrix and therefore increased Brownian term. Also it was observed that in 0.8 and higher porosities the effect of thermal conduction was decreased and the omission of Brownian term in these porosities resulted in less calculation errors. But in lower porosities and especially in porous matrix with lower heat ratios (insulated matrix), Brownian term should be considered in the calculations.

In the results it was observed that in lower Rayleighs the Brownian effect was very high and the value of Brownian term was decreased gradually by increasing Rayleigh which was due to faster nanofluid circulation and therefore higher viscosity effect inside the chamber. This phenomenon resulted in increased Nusselt factor in lower Rayleighs and decreased Nusselt factor in higher Rayleighs. Also the presence of the porous matrix resulted in changed temperature distribution and therefore changed Brownian values in different Rayleighs.

## References

- [1] D. Nield, A. Bejan, *Convection in Porous Media*, Third Ed, New York: Springer, 2006.
- [2] D. L. Youchison, B. E. Williams, R. E. Benander, (2011), Porous nuclear fuel element for high-temperature gas-cooled nuclear reactors, Patent No.: US 7,889,146 B1. Date of Patent: Mar. 1.
- [3] K. Vafai, *Porous Media: Applications in Biological Systems and Biotechnology*, New York, CRC Press, 2010.
- [4] M. Sheikholeslami, M. Gorji-Bandpy, D.D. Ganji, Soheil Soleimani, *Journal of the Taiwan Institute of Chemical Engineers*, 45 (2014) 40–49.
- [5] J. Koo, C. Kleinstreuer, *Journal of Nanoparticle Research*, 6 (2004) 577–588.
- [6] S.M. Aminossadati, B. Ghasemi, *International Communications in Heat and Mass Transfer*, 38 (2011) 672–678.
- [7] B. Ghasemi, S.M. Aminossadati, *International Journal of Thermal Sciences*, 49 (2011) 931-940.
- [8] M. H. Kayhani, M. Nazari, E. Shakeri, *Transp Porous Med*, 87 (2011) 625–633.
- [9] Sarita Pippal, P. Bera, *International Journal of Heat and Mass Transfer*, 56 (2013) 501–515.
- [10] L. R. Mealey, J. H. Merkin, *International Journal of Thermal Sciences*, 48 (2009) 1068-1080.
- [11] C. Beckermann, S. Ramadhyani, R. Viskanta, *Journal of Heat Transfer*, 109 (1987) 363-370.
- [12] S. B. Sathe, T. W. Tong, *Int. comm. heat mass transfer*, 15 (1988) 203-212.
- [13] M.A. Sheremet, I. Pop, *International Journal of Heat and Mass Transfer*, 79 (2014) 137–145.
- [14] M.A. Sheremet, I. Pop, M.M. Rahman, *International Journal of Heat and Mass Transfer*, 82 (2015) 396–405.
- [15] Q. Sun, I. Pop, *Int. J. Therm. Sci*, 50 (2011) 2141-2153.
- [16] M. Mahmoodi, S. MazroueiSebdani, *Superlattices and Microstructures*, 52 (2012) 261-275.
- [17] S. Ergun, *Chemical Engineering Progress*, 48 (1952) 89-94.
- [18] K. Khanafer, K. Vafai, M. Lightstone, *International Journal of Heat and Mass Transfer*, 46 (2003) 3639-3653.
- [19] J. Koo, C. Kleinstreuer, *Laminar nanofluid flow in microheat-sinks*, *International Journal of Heat and Mass Transfer*. 48 (2005) 2652–2661.
- [20] H. C. Brinkman, *Journal of Chemical Physics*, 20 (1952) 571-581.
- [21] J. C. Maxwell-Garnett, *Philosophical Transactions of the Royal Society A*, 203 (1904) 385–420.
- [22] H. F. Oztop, E. Abu-Nada, *International Journal of Heat and Fluid Flow*, 29 (2008) 1326–1336.
- [23] S.W. Patankar, *Numerical Heat Transfer and Fluid Flow*. New York: McGraw-Hill, 1980.
- [24] A. Zehforoosh, S. Hossainpour, *Mechanical Engineering*, 14 (2015) 34-44.